

## **Development of a multiplexing fingerprint and high wavenumber Raman spectroscopy technique for real- time *in vivo* tissue Raman measurements at endoscopy**

Mads Sylvest Bergholt  
Wei Zheng  
Zhiwei Huang

# Development of a multiplexing fingerprint and high wavenumber Raman spectroscopy technique for real-time *in vivo* tissue Raman measurements at endoscopy

Mads Sylvest Bergholt, Wei Zheng, and Zhiwei Huang

National University of Singapore, Optical Bioimaging Laboratory, Department of Bioengineering, 117576, Singapore

**Abstract.** We report on the development of a novel multiplexing Raman spectroscopy technique using a single laser light together with a volume phase holographic (VPH) grating that simultaneously acquires both fingerprint (FP) and high wavenumber (HW) tissue Raman spectra at endoscopy. We utilize a customized VPH dual-transmission grating, which disperses the incident Raman scattered light vertically onto two separate segments (i.e.,  $-150$  to  $1950\text{ cm}^{-1}$ ;  $1750$  to  $3600\text{ cm}^{-1}$ ) of a charge-coupled device camera. We demonstrate that the multiplexing Raman technique can acquire high quality *in vivo* tissue Raman spectra ranging from  $800$  to  $3600\text{ cm}^{-1}$  within  $1.0\text{ s}$  with a spectral resolution of  $3$  to  $6\text{ cm}^{-1}$  during clinical endoscopy. The rapid multiplexing Raman spectroscopy technique covering both FP and HW ranges developed in this work has potential for improving *in vivo* tissue diagnosis and characterization at endoscopy. © The Authors. Published by SPIE under a Creative Commons Attribution 3.0 Unported License. Distribution or reproduction of this work in whole or in part requires full attribution of the original publication, including its DOI. [DOI: [10.1117/1.JBO.18.3.030502](https://doi.org/10.1117/1.JBO.18.3.030502)]

Keywords: *in vivo*; endoscopy; Raman spectroscopy; multiplexing.

Paper 130001LR received Jan. 2, 2013; revised manuscript received Jan. 23, 2013; accepted for publication Feb. 11, 2013; published online Feb. 28, 2013.

Near-infrared (NIR) Raman spectroscopy is a vibrational analytic technique that can provide fingerprint (FP) information about the structure and conformation of tissues at the molecular level.<sup>1-3</sup> Very recently, NIR Raman spectroscopy techniques have gained considerable attention for characterization and diagnosis of precancer and cancer *in vivo* in a variety of organs such as head and neck,<sup>2</sup> cervix,<sup>3</sup> lung,<sup>4</sup> and gastrointestinal tracts.<sup>5,6</sup> To date, most NIR Raman studies have been centered on the FP range (i.e.,  $800$  to  $1800\text{ cm}^{-1}$ ) owing to the wealth of specific biomolecular information (i.e., protein, deoxyribonucleic acid,

and lipid content) contained in this spectral region for tissue characterization and diagnosis.<sup>5-7</sup> With the commonly used NIR  $785\text{ nm}$  laser excitation source, however, intense tissue autofluorescence background and fused silica Raman signal arising from fiber-optic Raman probes also fall into the FP range. The tissue autofluorescence can severely interfere with the detection of the inherently weak FP Raman signals by saturating the charge-coupled device (CCD). This remains the primary concern in certain organs such as lung, liver, and stomach.<sup>4,6</sup> Recent reports have shown that high wavenumber (HW) (i.e.,  $2800$  to  $3700\text{ cm}^{-1}$ ) Raman spectroscopy also contains valuable biomolecular information that can advantageously be used for diagnostic purposes.<sup>1-4,8,9</sup> The use of HW Raman spectroscopy is appealing due to the relatively intense tissue Raman signals generated ( $\text{CH}_2$  and  $\text{CH}_3$  moiety stretching vibrations of protein and lipids, OH stretching vibrations of water), as well as the considerably reduced fused silica fiber interferences and tissue autofluorescence that may allow a better assessment of the genuine tissue Raman signals.<sup>2,9</sup> Our study has established that the integrated FP and HW Raman technique offers complimentary diagnostic information for increasing the accuracy and robustness of detecting precancer in cervical tissue.<sup>8</sup> To date, only a very limited clinical work has been reported on the tissue Raman measurements covering both the FP and HW regions. The tissue Raman signals are measured either by successively switching the different laser excitation frequencies or by rotating the gratings for each spectral region,<sup>1,8</sup> which are not suitable for rapid *in vivo* measurements in clinical endoscopic settings. In this letter, we report on the development of a novel multiplexing Raman spectroscopic technique that can simultaneously acquire both FP and HW *in vivo* tissue Raman spectra with high spectral resolution during endoscopy.

Figure 1 shows the schematic of the multiplexing Raman spectroscopy system developed for simultaneous acquisition of the FP and HW Raman spectra in real-time under endoscopic image-guidance [i.e., white light reflectance (WLR), narrow-band imaging (NBI) and autofluorescence imaging (AFI)]. The multiplexing Raman spectroscopy technique consists of a spectrum stabilized  $785\text{ nm}$  diode laser (maximum output:  $300\text{ mW}$ , B&W TEK Inc., Newark, Delaware), a transmissive imaging spectrograph (Holospec f/1.8, Kaiser Optical Systems Inc., Ann Arbor, Michigan) equipped with a liquid nitrogen-cooled ( $-120^\circ\text{C}$ ), NIR-optimized, back-illuminated and deep depletion CCD camera ( $1340 \times 400$  pixels at  $20 \times 20\text{ }\mu\text{m}$  per pixel; Spec-10: 400BR/LN, Princeton Instruments, Roper Scientific Inc., Trenton, New Jersey). We integrate a customized volume phase holographic (VPH) dual-transmission grating consisting of two hybrid VPH gratings ( $1400$  and  $1600\text{ g/mm}$ ) (HoloPlex, Kaiser Optical Systems Inc., Ann Arbor, Michigan) into the spectrograph for Raman spectral dispersion.<sup>10</sup> The hybrid gratings are cemented closely together with a tilted angle of  $\sim 0.2$ -deg to achieve a separation between the low frequency and high frequency spectral components. The Bragg wavelengths of the hybrid gratings are tuned to two different spectral ranges (i.e.,  $-150$  to  $1950\text{ cm}^{-1}$  and  $1750$  to  $3600\text{ cm}^{-1}$ ) such that it disperses the tissue Raman spectra (i.e., FP and HW spectra) onto two separate vertical segments of the CCD, accordingly. This multiplexing Raman spectroscopy technique based on a VPH dual-transmission grating permits simultaneous coverage of both the FP and HW spectral segments while maintaining a high spectral resolution of a single high-density grating. To correct for the image aberration in the transmissive spectrograph,

Address all correspondence to: Zhiwei Huang, National University of Singapore, Optical Bioimaging Laboratory, Department of Bioengineering, 9 Engineering Drive 1, Singapore 117576. Tel: +65- 6516-8856; Fax: +65- 6872-3069; E-mail: [biehzw@nus.edu.sg](mailto:biehzw@nus.edu.sg)

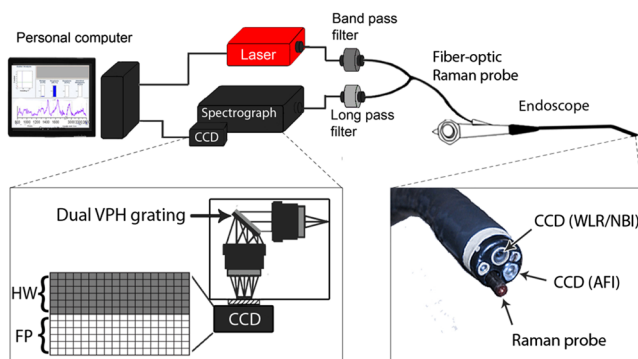


**Fig. 1** Schematic diagram of the rapid multiplexing Raman spectroscopy technique for simultaneous acquisition of both the fingerprint (FP) and high wavenumber (HW) Raman spectra under trimodal endoscopic imaging [i.e., white light reflectance (WLR), narrowband imaging (NBI), autofluorescence imaging (AFI)] guidance. A customized dual-transmission VPH grating is incorporated into the Raman system for dispersion of FP and HW Raman spectra onto different vertical segments of a CCD.

a customized parabolic aligned fiber bundle ( $26 \times 100 \mu\text{m}$  fibers,  $\text{NA} = 0.22$ ) was coupled into the entrance slit of the spectrograph for significantly improving the signal-to-noise ratio (SNR) as well as the spectral resolution of the multiplexing Raman system as compared to a conventional straight slit imaging spectrograph.<sup>7</sup> This allows us to completely hardware bin the two separate CCD segments vertically for improving the SNR (of up to  $\sim 14 (= 200^{1/2})$ ) and spectral resolution ( $3 - 6 \text{ cm}^{-1}$ ) of the Raman spectra.<sup>7</sup> The two spectral segments are simultaneously readout so that the FP and HW regions can be spliced into a complete high-resolution broadband Raman spectrum covering  $-150$  to  $3600 \text{ cm}^{-1}$ . The rapid multiplexing Raman spectroscopy technique developed for endoscopy was wavelength calibrated to an accuracy ( $\pm 2 \text{ cm}^{-1}$ ) using an argon/mercury spectral lamp (AR-1 and HG-1, Ocean Optics Inc., Dunedin, Florida) and the Raman spectrum of 4-acetamidophenol that exhibits strong well-defined peaks in the HW region at  $2931 \text{ cm}^{-1}$  and  $3064 \text{ cm}^{-1}$  (ASTM E1840 standard). To correct for the spectral response of the system, intensity calibration was performed using a standard tungsten lamp (RS-10, EG&G Gamma Scientific, San Diego, California) of the two distinct CCD segments separately. In this work, a 1.8 mm fiber-optic confocal Raman probe coupled with a 1.0 mm sapphire ball lens that can pass through the instrument channel of conventional endoscopes was used for epithelial tissue Raman measurements during endoscopic procedures. We have also developed customized software to process the two distinct CCD segments in real-time during clinical endoscopy, and the proper probe-tissue contact handlings can be verified on-line using outlier detection algorithms.<sup>11</sup> The real-time data processing specially developed for this biomedical multiplexing FP and HW Raman spectroscopy technique includes silica fiber background subtraction, intensity and wavelength calibration, cosmic rays and signal saturation detection/rejection, autofluorescence background subtraction and linear Savitzky-Golay smoothing (5 pixel window).<sup>5</sup> Different tissue autofluorescence background subtraction schemes were employed for robust extraction of the tissue Raman signals. In the FP region (i.e.,  $800$  to  $1800 \text{ cm}^{-1}$ ), a 5th order polynomial constrained to the lower portion of the FP Raman spectra is used and this polynomial is then subtracted from the measured spectrum to resolve the FP tissue Raman



**Fig. 2** Image of a parabolic arranged fiber bundle ( $26 \times 100 \mu\text{m}$ ,  $\text{NA} = 0.22$ ) illuminated with an argon/mercury lamp, illustrating the fully correction of image-aberration in spectrograph. The customized dual-transmission VPH grating efficiently disperses the FP and HW Raman spectra onto different vertical CCD segments. The lower segment covers the FP region  $-150$  to  $1950 \text{ cm}^{-1}$  (spectral resolution of  $6 \text{ cm}^{-1}$ ) while the upper segment covers the nonspecific Raman range and the HW range from  $1750$  to  $3600 \text{ cm}^{-1}$  (spectral resolution of  $3 \text{ cm}^{-1}$ ).

signal. In the HW region (i.e.,  $2800$  to  $3600 \text{ cm}^{-1}$ ), we found that 1st order polynomials constrained to the lower portion of the HW Raman spectra are optimal for extracting the Raman spectra. All Raman spectra are also normalized to the integrated areas under the FP and HW Raman spectral regions, respectively, to reduce power density fluctuations associated with probe handling variations during clinical endoscopic examinations.<sup>5,6</sup>

Figure 2 shows the full frame CCD image of a parabolic-configured fiber bundle illuminated with argon/mercury spectral lamps (AR-1 and HG-1, Ocean Optics Inc., Dunedin, Florida). With this specific fiber arrangement, the atomic emission lines are substantially straight, indicating effective image-aberration correction on the segmented CCD.<sup>7</sup> This in turn allows us to hardware bin the two well-defined CCD regions covering  $1340 \times 200$  pixels without compromising spectral resolutions or reducing the SNR ratio. The lower segment of the CCD array covers the FP region (i.e.,  $-150$  to  $1950 \text{ cm}^{-1}$ ), and we obtained a spectral resolution of  $\sim 6 \text{ cm}^{-1}$  over the entire FP range using the  $100 \mu\text{m}$  core diameter fibers. On the other hand, the upper segment of the CCD array covers the spectral range of  $1750$  to  $3600 \text{ cm}^{-1}$  comprising the nonspecific Raman region ( $\sim 1800$  to  $2800 \text{ cm}^{-1}$ ) and the HW spectral region (i.e.,  $2800$  to  $3600 \text{ cm}^{-1}$ ) with a spectral resolution of  $\sim 3 \text{ cm}^{-1}$ . Since the dispersion is holographically encoded in the grating for both FP and HW spectral regions, the signal magnitude and resolution of a single high-density grating are essentially maintained.

We have illustrated the utility of the rapid multiplexing Raman spectroscopy system for real-time *in vivo* Raman measurements of epithelial tissue under wide-field endoscopic imaging (i.e., WLR/NBI/AFI) guidance. Figure 3 shows an example of *in vivo* Raman spectra acquired from different anatomical sites in the head and neck (i.e., attached gingiva, buccal mucosa, dorsal tongue, hard palate, and oropharynx) from a healthy volunteer under endoscopic imaging guidance. The FP and HW *in vivo* tissue Raman spectra can be acquired simultaneously with an integration time of  $0.5 \text{ s}$  and presented on the Raman endoscopy monitor in real-time. Highly resolved tissue Raman peaks in the head and neck are observed in the FP range with tentative molecular assignments<sup>2,3,6,8</sup> as follows:  $853 \text{ cm}^{-1}$  ( $\nu(\text{C}-\text{C})$  proteins),  $956 \text{ cm}^{-1}$  ( $\nu_s(\text{P}=\text{O})$  of hydroxyapatite),  $1004 \text{ cm}^{-1}$  ( $\nu_s(\text{C}-\text{C})$  ring breathing of phenylalanine),  $1078 \text{ cm}^{-1}$  ( $\nu(\text{C}-\text{C})$  of lipids),  $1265 \text{ cm}^{-1}$  (amide III  $\nu(\text{C}-\text{N})$  and  $\delta(\text{N}-\text{H})$  of proteins),  $1302 \text{ cm}^{-1}$  ( $\text{CH}_3\text{CH}_2$  twisting and wagging of proteins),  $1445 \text{ cm}^{-1}$  ( $\delta(\text{CH}_2)$  deformation of proteins and lipids),  $1655 \text{ cm}^{-1}$  (amide I  $\nu(\text{C}=\text{O})$  of proteins),

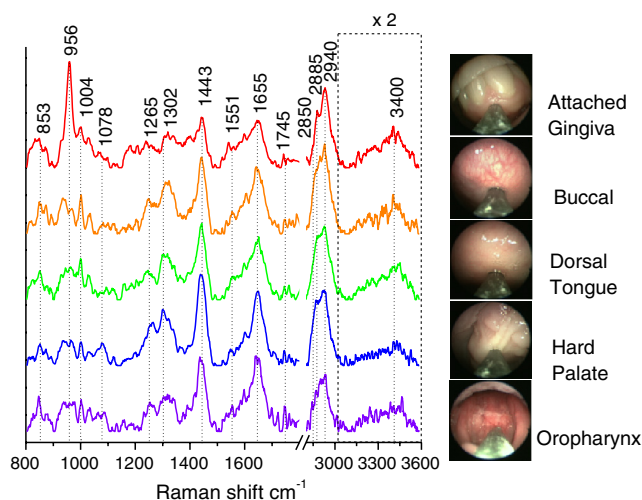


**Fig. 3** Example of *in vivo* Raman spectra acquired from different tissue sites (i.e., attached gingiva, buccal mucosa, dorsal tongue, hard palate and oropharynx) in the oral cavity from a healthy volunteer using the multiplexing Raman spectroscopy technique under endoscopic imaging guidance. The spectra are shifted vertically and normalized to the integrated areas in the FP and HW regions, respectively, for better comparisons of line shapes. All Raman spectra are acquired using an integration time of 0.5 s under the 785 nm illumination power of 1.5 W/cm<sup>2</sup>. *In vivo* fiber-optic Raman endoscopic acquisitions under WLR imaging guidance are also shown.

and 1745 cm<sup>-1</sup>  $\nu(\text{C}=\text{O})$  of lipids. Intense Raman peaks are also seen in the HW region such as 2850 and 2885 cm<sup>-1</sup> (symmetric and asymmetric CH<sub>2</sub> stretching of lipids), 2940 cm<sup>-1</sup> (CH<sub>3</sub> stretching of proteins) as well as the broad Raman band of water (OH stretching vibrations that peak at 3400 cm<sup>-1</sup> in the 3100 to 3600 cm<sup>-1</sup> region). One notes that some tissue Raman signals (e.g., 956 cm<sup>-1</sup> ( $\nu_s(\text{P}=\text{O})$  of hydroxyapatite) of hard palate) observed using the fiber-optic confocal Raman probe in this study slightly deviate from our preceding oral tissue Raman spectra using a rigid ball-lens Raman probe.<sup>12</sup> The discrepancies related to bone Raman signals below the masticatory mucosa could be attributed to the shallower tissue probing depth by using the fiber-optic confocal Raman probe suited for superficial epithelial tissue measurements in this work. The approximate SNR of 25 could be obtained from *in vivo* tissue Raman spectra at 1445 cm<sup>-1</sup> using 1.0 s integration time when the fiber-optic confocal Raman probe is in gentle contact with the buccal mucosa. Although the Raman band of water observed was relatively noisy due to the low quantum efficiency above 1090 nm of the CCD camera used, it may still contain important diagnostic information related to the local conformation and interactions of hydrogen-bonds in the cellular and extracellular space of tissue.<sup>2,3,8,13</sup> The OH stretching vibrations have been found to be associated with aquaporins and protein/water interactions in precancer and cancer tissues.<sup>2,3,8</sup> Therefore, compared with either FP or HW Raman spectroscopy technique alone, the multiplexing Raman spectroscopy technique utilizing a single excitation laser source together with a VPH dual-transmission grating provides both the FP and HW Raman spectra simultaneously (including OH stretching vibrations of water) with high spectral resolution (i.e., 3 to 6 cm<sup>-1</sup>), paving the way for an improved tissue diagnosis and characterization *in vivo*.<sup>8</sup> The instrumentation development in biomedical spectroscopy reported in this work is of particular importance for Raman endoscopic applications that require rapid tissue Raman

measurements in a broad spectral range without switching between different excitation laser sources or rotating the grating back and forth, as well as for those internal organs (e.g., gastric, liver, and lung) that exhibit intense tissue autofluorescence interference in the FP region but require HW Raman measurements. Currently, *in vivo* FP/HW Raman measurements on a larger series of patients are in progress to evaluate the clinical merits of the multiplexing Raman spectroscopy technique for improving *in vivo* diagnosis and characterization of early cancer in the head and neck during clinical endoscopy.

In conclusion, we report on the development of a novel multiplexing Raman spectroscopy technique for simultaneous acquisition of the FP (800 to 1800 cm<sup>-1</sup>) and HW (2800 to 3600 cm<sup>-1</sup>) tissue Raman spectra *in vivo* with high spectral resolution (3 to 6 cm<sup>-1</sup>). We demonstrate that high quality *in vivo* Raman spectra ranging from 800 to 3600 cm<sup>-1</sup> of different tissue sites in the head and neck can be measured within 1.0 s integration time during endoscopic examination. The rapid multiplexing Raman spectroscopy technique with high spectral resolution developed in this work opens the opportunity for improving real-time *in vivo* tissue Raman diagnosis and characterization at endoscopy.

### Acknowledgments

This research was supported by the National Medical Research Council, and the Biomedical Research Council, Singapore.

### References

1. H. Chau et al., "Fingerprint and high-wavenumber Raman spectroscopy in a human-swine coronary xenograft *in vivo*," *J. Biomed. Opt. Lett.* **13**(4), 040501 (2008).
2. K. Lin, D. Lau, and Z. Huang, "Optical diagnosis of laryngeal cancer using high wavenumber Raman spectroscopy," *Biosens. Bioelectron.* **35**(1), 213–217 (2012).
3. J. Mo et al., "High wavenumber Raman spectroscopy for *in vivo* detection of cervical dysplasia," *Anal. Chem.* **81**(21), 8908–8915 (2009).
4. M. A. Short et al., "Using laser Raman spectroscopy to reduce false negatives of autofluorescence bronchoscopies," *J. Thorac. Oncol.* **6**(7), 1206–1214 (2011).
5. Z. Huang et al., "Integrated Raman spectroscopy and trimodal wide-field imaging techniques for real-time *in vivo* tissue Raman measurements at endoscopy," *Opt. Lett.* **34**(6), 758–760 (2009).
6. M. S. Bergholt et al., "Fiber-optic Raman spectroscopy probes gastric carcinogenesis *in vivo* at endoscopy," *J. Biophoton.* **6**(1), 49–59 (2013).
7. Z. Huang and H. Zeng, "Rapid near-infrared Raman spectroscopy system for real-time *in vivo* skin measurements," *Opt. Lett.* **26**(22), 1782–1784 (2001).
8. S. Duraipandian et al., "Simultaneous fingerprint and high wavenumber confocal Raman spectroscopy enhances early detection of cervical precancer *in vivo*," *Anal. Chem.* **84**(14), 5913–5919 (2012).
9. S. Koljenovic et al., "Tissue characterization using high wave number Raman spectroscopy," *J. Biomed. Opt.* **10**(3), 031116 (2005).
10. H. Owen, "The impact of volume phase holographic filters and gratings on the development of Raman instrumentation," *J. Chem. Educ.* **84**(1), 61–66 (2007).
11. S. Duraipandian et al., "Real-time biomedical Raman spectroscopy for *in vivo*, on-line gastric cancer diagnosis during clinical endoscopic examination," *J. Biomed. Opt.* **17**(8), 081418 (2012).
12. M. S. Bergholt, W. Zheng, and Z. Huang, "Characterizing variability in *in vivo* Raman spectroscopic properties of different anatomical sites of normal tissue in the oral cavity," *J. Raman Spectrosc.* **43**(2), 255–262 (2012).
13. L. Carvalho et al., "Diagnosis of inflammatory lesions by high-wavenumber FT-Raman spectroscopy," *Theor. Chem. Acc.* **130**(4–6), 1221–1229 (2011).